Study of a Water Electrolysis System using a Compact Solar Cell Module with a Plant Shoot Configuration *

Shin'ya OBARA**

**Department of Electrical and Electronic Engineering, Kitami Institute of Technology
165 Koen-cho, Kitami, Hokkaido 090-8507, Japan
E-mail: obara@mail.kitami-it.ac.jp

Abstract

The system proposed in this paper produces hydrogen by supplying photovoltaic power to a water electrolyzer and then supplying this gas to a fuel cell with a time shift. The objective of this system is to supply power to an individual house or apartment building with only green energy. However, the solar cell module installation area is large in the proposed system. Therefore, this paper considered installing a solar cell module with a plant shoot configuration. As a result of this modification, the power generation area of the proposed system is 33% to 52% smaller than that of a conventional flat solar cell module. From these results, it is possible to introduce the proposal system into an individual house.

Keywords: Water electrolysis, Solar power, Plant shoot arrangement, Energy volume density, Genetic algorithm, Ginkgo biloba.

1. Introduction

The ultimate goal of a fuel cell system is to operate using hydrogen produced by green energy. Hydrogen production technology using green energy includes, e.g., electrolyzing water using wind power or solar power. In addition, there are a few example water electrolysis systems that use photovoltaic power generation [1-3]. In the proposed system, all of the power of a house is supplied with a small fuel cell using the hydrogen obtained from water electrolysis by photovoltaic power. Hydrogen and oxygen formed by water electrolysis are stored in each cylinder. These gases can be supplied to a fuel cell over time. However, this system is expensive. In particular, the cost of a fuel cell, water electrolyzer, and solar cell will greatly influence the spread of the system. The equipment cost of the present fuel cell can easily be estimated. Moreover, a highly efficient water electrolyzer has yet to be developed [4-6]. On the other hand, the facility cost (i.e., solar cell area) of a photovoltaics is influenced by the installation location (latitude and longitude) and installation requirements (the angle of direction and the angle of elevation) of the system. Therefore, it is necessary to know the solar cell area installed into the proposed system. In this paper, the amount of hydrogen consumed by the PEFC (proton-exchange membrane fuel cell) is calculated from the daily electricity demand of a house. Moreover, the solar cell area required to obtain this amount of

hydrogen is clarified. Based on the efficiency of a water electrolyzer, a fuel cell, and a compressor, it is expected that the solar cell area is too large for the existing photovoltaic system. When the solar cell area is large, it is difficult to install the proposed system in an urban area. Consequently, in order to reduce the installation area of the solar cell, a solar cell module is installed with a plant shoot configuration (similar to the stalk, stem of a leaf, and leaf on a plant). Generally, the light that reaches a plant leaf is separated into a reflective component, an absorption component to the chloroplast, and a transmission component [7, 8]. A plant will not see its branches and leaves increase when in a low position, virtually inaccessible to sunlight. This configuration is remarkable as the individual in a stock [9]. Furthermore, the photosynthetic ability and respiration rate of leaves reached easily by sunlight increase. The received light characteristics of a plant shoot have been studied by morphological botany [10, 11]. However, there are a few examples that investigate the received light characteristics of the plant shoot configuration using numerical simulation. Therefore, Obara developed an simulation algorithm concerning optimization of the received light characteristics of a plant shoot [12-14]. They clarified the relationship between the received light characteristics and the plant shoot configuration, such as that of a ginkgo biloba, using this simulation program [12-14]. From these research findings, it is thought that a solar cell module with a plant shoot configuration of lobed leaves, such as that of ginkgo biloba, reduces the installation area greatly compared to that of a conventional flat solar cell module.

The objectives of this study are to introduce a solar cell module with the shoot configuration of ginkgo biloba into an individual house and to develop an independent electrical power system via utilization of solar energy. If the proposed system is confirmed according to the results of this study, a house with an independent green energy source is possible.

2. System Configuration

2.1 System operation

(1) Solar module

Figure 1 shows an energy supply system with a fuel cell, a photovoltaics and a water electrolyzer. A flat solar cell module requires a wide installation area. However, because it is difficult to obtain a wide area near a house or apartment in an urban area, installation of the solar cell is limited. Therefore, this paper considers installation of a solar cell module with a plant shoot configuration. The details of this module are described in Section 3. Solar cell power is supplied to the water electrolyzer and the demand side through an inverter.

(2) Water electrolyzer and gas cylinder

The power exceeding the demand load of the solar cell is supplied to the water electrolyzer. The hydrogen and oxygen from the water electrolyzer are stored in a cylinder through a compressor. The gases from these cylinders can be supplied to the fuel cell at an arbitrary time by opening and closing a control valve.

(3) Fuel cell power

The hydrogen and oxygen in each cylinder are supplied to a PEFC. The PEFC power is supplied to the demand side through an inverter. The exhaust heat of the PEFC is stored in a heat storage tank. The heat demand side is supplied by the heat storage tank or by reheating the boiler.

2.2 PEFC

A PEFC performance shown in Fig. 2 is introduced in this paper [12, 13]. In the proposed system, pure hydrogen and pure oxygen are supplied to the PEFC. Therefore, cell performance is improved relative to the supply of reforming gas and air. Cell performance improvements include an increase in the output characteristics and improvements in the partial-load characteristics. In the following simulation, the power generation efficiency of the fuel cell is set to 55% [15, 16]. Therefore, there is no decrease in PEFC efficiency under partial-load operation.

2.3 Water electrolyzer

The hydrogen production $Q_{el,j,H_2,st}$ in the water electrolyzer j from sampling time st to $st+1$ is calculated via the following formula using the electric power consumption $\Delta E_{el,j,st}$ and efficiency φ_{el} of the water electrolysis. Moreover, j is the installed water electrolyzer number, and area A_j is the surface area of an electrode. Although φ_{el} changes with the type of water electrolyzer, $\Delta E_{el,j,st}$ and φ_{el} are set to 80% in the following simulation example.

$$Q_{el,j,H_2,st} = \frac{\Delta E_{el,j,st} \cdot A_j}{D \cdot Y_j} \cdot \varphi_{el} \tag{1}$$

2.4 Compression storage of hydrogen and oxygen gas

After hydrogen and oxygen from the water electrolyzer are pressurized with compressors, they are stored in cylinders. The compressor work is assumed to be compression work of an ideal gas and is calculated by Eq. (2). φ_c is the whole compressor efficiency. Power consumption in an inverter and an electric motor, transfer loss of power, loss with insufficient air leak and cooling, and other mechanical loss are included in φ_c. In the following simulation, φ_c is set to 50%as in a real machine.

$$L_{c,H_2,st} = P_\infty \cdot U_{\infty,st} \cdot \ln(P_{c,H_2} / P_\infty) / \varphi_c \tag{2}$$

3. Solar Cell Module with a Plant Shoot Configuration

3.1 Configuration of plant shoots

It is thought that many kinds of plants have evolved so that the photosynthetic rate may be maximized. Because the biomass is produced from photosynthesis, top priority is given to the configuration evolution of the leaf, which influences the amount of light a plant receives. Generally, the light that reaches a plant leaf is separated into a reflective component, an absorption component

to the chloroplast, and a transmission component. Therefore, the optimal arrangement of the leaves to maximize the amount of light receives is investigated by introducing a Genetic Algorithm (GA). A plant in a community evolves to obtain as much solar radiation as possible. Therefore, a very compact light-receiving system may be able to be designed by mimicking a plant. In this paper, a solar cell module with the shoot configuration of ginkgo biloba is introduced. However, a plant shoot configuration is strongly related to the solar position and the amount of solar radiation (Fig. 3). In this study, the light-receiving characteristics of a ginkgo biloba shoot are investigated, and a solar cell module with a weak directive and small installation area is proposed. When this solar cell module is introduced into the proposed system, it is predicted that the amount of hydrogen production by water electrolysis increases.

3.2 Simulation method of the amount of light received

(1) Coordinate system and virtual radiation plate

The simulation method to determine the amount of light received in a ginkgo biloba shoot configuration is described below. The simulation coordinate system concerning the plant shoot model is shown in Fig. 4. The x-coordinate is directed south, and the y-coordinate faces east. The $x-y$ plane is a level surface, and the z-axis is perpendicular to the level surface. Each leaf model is movable to a free position. However, in this paper, the length of each leaf branch is defined beforehand and the edges of these branches are always joined to the centre of the coordinate system.

Solar radiation (direct solar radiation) is emitted perpendicularly to the arbitrary points of view on the virtual radiation plate. However, the normal line through the central point of the virtual radiation plate always passes along the centre of the coordinate system. The distance between the virtual radiation plate and the centre of the coordinate system is given by l_{rd}. Here, l_{rd} is separated from the plant shoot. The magnitude of the virtual radiation plate causes the emitted rays to cover the whole leaf model.

(2) Coordinates of a plant shoot model

Figures 5 (a) and (b) illustrates the procedure to determine the coordinates of the ginkgo biloba shoot model. First, as shown in Fig. 5 (a), the shoot model is set at position L0. Here, movement of the coordinate $P_{L0}(X, Y, Z)$ of the base point of the leaf in Figs. 5 (a) and (b) is described as an example. Rotation of the angle of elevation $\phi_{a,i}$ (i is a number of a leaf) about the x-axis is added for P_{L0}. The position of the plant shoot model is position L1 in Fig. 5 (a), and P_{L0} moves to $P_{L1}(x', y', z')$. Next, rotation of the angle of direction $\theta_{a,i}$ about the z-axis is added for the plant shoot model. The position of the plant shoot model at this time is position L2 in Fig. 5 (b), and P_{L1} moves to $P_{L2}(x'', y'', z'')$. Finally, the angle of rotation $\alpha_{a,i}$ is added to the radial direction of the branch of a leaf (position L3 in Fig. 5 (b)).

(3) The shoot model of ginkgo biloba

The leaf model of ginkgo biloba is shown in Figs. 5 (c) and (d). The branch of a leaf with length $r_{a,i}$ (i is a number of a leaf) is fixed to the leaf model. This leaf model consists of 97 surface

elements. The apex coordinate $P_{a,n,m}$ (n is a surface element number and m is an apex number) of each surface element is expressed as the distance $l_{a,n,m}$ between the base point of the leaf in Fig. 5 (d) and the angle $\varepsilon_{a,n,m}$ with the base line that passes along the base point of the leaf. All of the surface elements are defined by the set of $l_{a,n,m}$ and $\varepsilon_{a,n,m}$ (n=97, m=1, 2, 3, 4).

(4) Objective function and chromosome model

Maximization of the amount of light received per day by a plant shoot is set as an objective function. This objective function is used as input to a genetic algorithm (GA). Figure 6 shows the chromosome model used by the GA. The chromosome model is expressed as a value of 0 or 1 with 10 bits $\theta_{a,i}$, $\phi_{a,i}$, and $\alpha_{a,i}$, as shown in Figs. 5 (a) and (b). When a real number is expressed with a 10-bit binary number, the simulation error is 1% or less. Here, subscript i expresses the leaf number of a plant shoot, and J_l is the total number of leaves of the shoot. An initial generation's chromosome model is decided using random numbers. The solution with high adaptive value (same objective function value) is obtained by repeating a generation while adding genetic manipulation.

3.3 Simulation procedure of the amount of light received

The simulation calculation flow is shown in Fig. 7. The shape data (Figs. 5 (c) and (d)) of the leaf model, the generation number, and the GA parameter are input first. Next, the initial generation of chromosome models is generated at random, as shown in Fig. 6. By decoding these chromosome models, the coordinates of the shoot shown in Figs. 4, 5 (a) and 5 (b) are obtained. Moreover, a Monte Carlo calculation determines the emission position $P_{d,l}$ (l is the number of rays to emit) of the light quantum on the virtual radiation plate. The ray trajectory can be determined by calculating the normal line vector of the light quantum. The number of rays to emit is calculated based on the amount of solar radiation in each hour of a representative day. Furthermore, the position of the virtual radiation plate changes for each sampling hour to simulate the position of the sun, as shown in Fig. 3 (a). Chromosome models with more ray-absorbing leaves are considered to be solutions with high adaptive value. A genetic mutation is added to the chromosome group with high adaptive value, a new random chromosome is added to a group, and the next-generation chromosome group is generated. Repeated calculations are carried out based on the last generation number given beforehand. In the last generation's chromosome model group, the individual with the highest adaptive value is considered to be the optimal solution. The optimal arrangement of a ginkgo biloba shoot can be obtained by decoding this chromosome model.

3.4 Number of rays emitted from the virtual radiation plate

In the sampling time st of the representative month g, the ray number $nq_{g,st}$ emitted from the virtual radiation plate is calculated using Eq. (3). However, N_a is the total number of light quanta emitted from the virtual radiation plate on a representative day, and $R_{g,st}$ is a rate of the number of light quanta emitted on st. In addition, $e_{g,st}$ is the amount of horizontal plane global solar radiation in the hour st of the representative month g.

$$nq_{g,st} = N_a \cdot R_{g,st} = N_a \cdot \left(e_{g,st} \Big/ \sum_{st=0}^{Day} e_{g,st} \right) \tag{3}$$

The position of the virtual radiation plate is set as the solar position (the angle of direction θ_s and the elevation angle ϕ_s), as shown in Fig. 3 (a), and this position changes every hour. The values in Fig. 3 (b) are used for $e_{g,st}$. Calculating the number of rays emitted by the virtual radiation plate from Eq. (3) in the case of $N_a = 10000$ generates the result in Fig. 8. The simulation procedure gives details to reference [17].

4. Simulation Method

4.1 Assumption of the proposed system

The proposed system (Fig. 1) is simulated in an individual house. Equation (4) is a power balance equation of the proposed system at sampling time st

$$P_{s,st} + P_{f,st} = \Delta P_{d,st} + \Delta P_{e,st} + \Delta P_{l,st} \tag{4}$$

$P_{s,st}$ and $P_{f,st}$ are the electric power of a solar cell and a fuel cell, respectively. $\Delta P_{d,st}$ and $\Delta P_{e,st}$ are the electric power consumption of the electricity demand and water electrolyzer, respectively. Here, $\Delta P_{e,st}$ is equivalent to $\Delta E_{el,j,st}$ as described in Section 2.3. $\Delta P_{l,st}$ is the power consumed with a power conditioner (inverter) and a gas-compressor. In the simulation, the efficiency of the power conditioner is set to 95%, and the electric power consumption of the gas-compression is calculated by the method described in Section 2.4. Here, the hydrogen and oxygen cylinder pressure is set to 0.5 MPa. Details of the electricity demand $\Delta P_{d,st}$ are described in the next Section.

The electric power of the plate type solar cell (the conventional method) $P_{s,st}$ is calculated using the solar radiation slope [18], and the efficiency of the solar module. On the other hand, $P_{s,st}$ of a solar cell module with a plant shoot configuration is obtained by simulating the amount of light received by the method described in Section 3. Here, the equipment efficiency used for each simulation is shown in Table 1.

4.2 Amount of electricity demand and solar cell module area

Figure 9 shows the electricity demand pattern of a representative day every month for a standard house in Sapporo, Japan [19]. In this figure, the power demand pattern does not change significantly each month shown in Figs. 9 (b) and (c); this is because there is no cooling load in the summer in Sapporo. The electricity demand includes household appliances and electric lighting. Heat demand comes from heating, hot water supply and baths. The values of Fig. 9 are used for $\Delta P_{d,st}$ in Eq. (4). Because Sapporo is a cold, snowy area, a cooling load is not included in Fig. 9. On

the other hand, because hot water is used for heating, the heating load is not included in Fig. 9. The area of a solar cell module is calculable from $P_{s,st}$ when Eq. (4) is satisfied.

5. Simulation Results

5.1 Relationship between plant shoot configuration and the amount of light received

In order to investigate the received-light characteristics of the shoot configuration of a ginkgo biloba, the received-light characteristics of the square surface shown in Fig. 10 (a) are examined first. The length of a branch of a leaf gives three patterns of $r_{t,1}$ (0, 20, 40, 60 mm), $r_{t,2}$ (0, 30, 60, 90 mm), and $r_{t,3}$ (0, 50,100,150 mm). The parameters shown in Table 2 are used in GA. Figure 10 (b) shows the simulation result of the received-light density of the square surface. The light received density of the square surface is influenced by the ray trajectory based on the result in Fig. 10 (b). However, the received-light density is not influenced by the length of a branch of a leaf. Fig. 11 shows the simulation result of an acceptance surface with the shoot configuration of a ginkgo biloba under the same conditions. In this simulation, the leaf model of a ginkgo biloba shown in Fig. 5 (c) and (d) was installed with four leaves. Moreover, in order to investigate the received-light characteristics, the leaf model of a ginkgo tree with some area was calculated. From the results in Figs 11 (a) and (b), the received-light density with the ginkgo biloba configuration is influenced by the ray trajectory, the size of the leaf model, and the length of a branch of a leaf. This is because more light reaches a back leaf model with a ginkgo tree shoot configuration compared with a shoot of the square surface leaf. Accordingly, it is thought that a plant with divided leaves is designed as a ginkgo tree so that a high received-light density may be obtained. In the following simulation, the combination of the length of a branch of a leaf is $r_{t,2}$ (0, 30, 60, 90 mm), and the area of one leaf model is 25.5 cm^2.

5.2 Area of solar cell module

Table 3 is a result of the solar cell module area of each type. A flat solar cell module of level installation is a horizontal table. A flat solar cell module for the south has an angle of elevation of 30 degrees, and is considered a sloped area. A plant shoot configuration includes a solar cell module with the shoot configuration of a ginkgo biloba. From the result of Table 3, the area of the solar cell module in January is large through July. This is because there is greater solar radiation in July, as Fig. 3 (b) shows. The horizontal area of the solar cell module in July is smaller compared with the sloped area. Because the solar altitude in July is high, the horizontally installed solar cell module is more advantageous. The area of the solar cell module with the plant shoot configuration is the smallest. This result is an effect of the optimized arrangement of a solar cell module with the ginkgo biloba shoot configuration.

5.3 Operation result of the proposal system

Figure 12 show the operation results of the proposed system in January and July, respectively. Figures 12 (a) and 12 (e) show the load factor of the PEFC in each month. During daytime, the

photovoltaic power exceeds the amount demanded. Operation of PEFC stops in this time zone. Moreover, the load factor of PEFC, other than a short time zone in the evening is small. Figures 12 (b) and (f) show the solar cell electricity production with horizontal area and sloped area. The electricity production with a sloped area is slightly larger than that with horizontal area in January. The power, excluding the amount of electricity demand from the production of electricity of the solar cell of Figs. 12 (b) and (f), is used for hydrogen and oxygen production by the water electrolyzer. As a result, the power storage shown in Figs. 12 (c) and (g) is realized. These gas stores at 24:00 correspond to operation of the fuel cell on the next day. Furthermore, Figs. 12 (d) and (h) show the compressor power consumption while hydrogen and oxygen are being stored in cylinders.

5.4 Planning of solar cell module with ginkgo biloba shoot configuration

Figure 13 shows the simulation result of the solar cell module with the plant shoot configuration. Figures 13 (a) and (b) show the result of the electricity production and power storage with hydrogen and oxygen. The area of the solar cell module with the plant shoot configuration corresponds is 33% to 52% smaller than those of other types. From this result, the received-light density has improved greatly compared with the conventional plate type module by optimally arranging a solar cell module with a plant shoot configuration.

Figure 14 shows the optimal configuration of the solar cell module with the plant shoot configuration. The size of the leaf was fixed in these simulations. Moreover, the combination of the length of a branch of a leaf is also fixed. When changing these values, a smaller module arrangement is obtained. For example, when the model area of Fig. 5 (c) is set up ten times, l_w of Fig. 5 (d) is nearly 80 cm. The numbers of solar cell modules with a plant shoot configuration are 58 modules and 36 modules in January and July, respectively. The solar cell system with the plant shoot configuration of a ginkgo biloba consists of eight modules per set (mirror symmetry of four modules). In this case, eight systems (Fig. 14 (a)) are required in January, and five systems (Fig. 14 (b)) are required in July. On the other hand, for the configuration of a solar cell system with the plant shoot configuration, various compositions are obtained based on the size of a leaf model, the number of the modules installed in one system, and the combination of the length of a branch of a leaf. Based on the representative day of the smallest month of the amount of solar radiation, it is necessary to determine the module composition in an actual system.

From the result described in the top, the solar cell module with a ginkgo biloba shoot configuration can be installed in a narrower space compared with the conventional plate module. Moreover, installation of the proposed system in an individual house is a possibility based on the results shown in Figs. 12 and 13. It is necessary to discuss the trend of equipment cost independently.

6. Conclusions

In the proposed system, photovoltaic power is supplied to a water electrolyzer, and hydrogen and oxygen are produced. All of the power required for an individual house is supplied through the production of electricity by a PEFC with these gases. System operation was investigated using numerical simulation. Hydrogen and oxygen are stored in cylinders and can be used for arbitrary times. However, when the installation area of a solar cell is large, system installation in an urban area is difficult. Therefore, this paper investigated installation of a solar cell module with a ginkgo biloba shoot configuration (plant shoot configuration) in order to reduce the solar cell installation area. The areas of three horizontal solar cell modules (a flat solar cell module of level installation), the sloped solar cell modules (a flat solar cell module for south set as the angles of elevation 30 degree), and cells with a plant shoot configuration were discussed using numerical simulation on each representative day in January and July in Sapporo. As a result, it is demonstrated that the received-light density improved for the solar cell module with a plant shoot configuration compared with the conventional plate types. The area of the solar cell module with the plant shoot configuration is 33% to 52% that of other types. Moreover, it is expected that installation of the proposed system in an individual house is possible. However, equipment cost must continue to be investigated.

7. Nomenclature

A : electrode area (m^2)
D : the number of Faraday (96500C/mol) (C/kg)
ΔE : electric power consumption (kW)
e : the amount of horizontal plane global solar radiation
J_l : the total number of the leaves
L : work (J)
l_a : distance between the base point of the leaf model and the surface element apex (Fig. 6 (b)) (mm)
N_a : the total number of light quanta emitted in a day
nq : the number of light quanta to emit
P_a : point in the coordinate system
P_c : compressed pressure (Pa)
P_d : emission position on the virtual radiation surface concerning direct solar radiation
P_f : power of a fuel cell (kW)
P_s : power of a solar cell (kW)
P_∞ : atmosphere pressure (Pa)
ΔP_d : power consumption of the electricity demand (kW)
ΔP_e : power consumption of the water electrolyzer (kW)
ΔP_l : power consumption of the power conditioner (kW)
Q : quantity of flow (kg/s)
$R_{g,st}$: the rate emitted to st among N_a
r_t : length of a branch of a leaf (mm)
U_∞ : volume rate of flow at atmosphere pressure (m^3/s)
Y : the number of the auxiliary devices which consume electric power

Roman character

a_a : angle of rotation of the leaf model (degree)

ε_a : angle indicating the surface element apex on the leaf model (Fig. 6 (b)) (degree)
ϕ_a : angle of elevation of the leaf model (degree)
φ efficiency (%)
θ_a : angle of direction of the leaf model (degree)

Subscript
c : compressor
el : water electrolysis
g : representative month
m : apex number of the surface element of the leaf model
n : surface element number of the leaf model
s : sun
st : sampling time

Acknowledgments

This work was partially supported by a Grant-in-Aid for Scientific Research (C) from JSPS.KAKENHI (20560204).

References

[1] Thomas L. Gibson, Nelson A. Kelly. Optimization of solar powered hydrogen production using photovoltaic electrolysis devices. International Journal of Hydrogen Energy 2008; 33(21): 5931-5940.

[2] D. Dini. Hydrogen production through solar energy water electrolysis. International Journal of Hydrogen Energy 1983; 8(11): 897-903.

[3] Nelson A. Kelly, Thomas L. Gibson, David B. Ouwerkerk. A solar-powered, high-efficiency hydrogen fueling system using high-pressure electrolysis of water: Design and initial results. International Journal of Hydrogen Energy 2008; 33(11): 2747-2764.

[4] N. Nagai, M. Takeuchi, T. Kimura and T. Oka. Existence of optimum space between electrodes on hydrogen production by water electrolysis. International Journal of Hydrogen Energy 2003; 28(1): 35-41.

[5] S.A. Grigoriev, V.I. Porembsky and V.N. Fateev. Pure hydrogen production by PEM electrolysis for hydrogen energy. International Journal of Hydrogen Energy, 2006; 31(2):171-175.

[6] S. Sawada, T. Yamaki, T. Maeno, M. Asano, A. Suzuki, T. Terai and Y. Maekawa. Solid polymer electrolyte water electrolysis systems for hydrogen production based on our newly developed membranes, Part I: Analysis of voltage–current characteristics. Progress in Nuclear Energy 2008; 50(2-6): 443-448.

[7] Chelle, M. Could plant leaves be treated as Lambertian surfaces in dense crop canopies to estimate light absorption ?. Ecological Modeling 2006; 198: 219-228.

[8] Lenk, S. and Buschmann, C. Distribution of UV-Shielding of the Epidermis of Sun and Shade Leaves of the Beech (Fagus Sylvatica L.) as Monitored by Multi-Colour Fluorescence Imaging, J. Plant Physiology 2006; 163: 1273-1283.

[9] Takenaka, A. A Simulation Model of Tree Architecture Development based on Growth Response to Local Light Environment. J. Plant Research 1994; 107: 321-330.

[10] The Society for the Study of Species Biology, Figures of Light, Water, and a Plant-Guide to Plant Physiological Ecology, Bun-ichi Sogo Shyuppan, Tokyo, Japan; 2003 (In Japanese)
[11] Hirose. T., Werger, M. J. A., Pons, T. L. and Rheenen, J. W. A. Canopy Structure and Leaf Nitrogen Distribution in a Stand of Lysimachia Vulgaris L. as Influenced by Stand Density, Oecologia 1988; 77.
[12] Shin'ya Obara. Influence of Diffused Solar Radiation on the Solar Concentrating System of a Plant Shoot Configuration. Journal of Thermal Science and Technology 2009; 4(2): 272-283.
[13] Shin'ya Obara. Study of the Light Received Characteristics of a Plant-Shoot-Condensing System with Simple Leaves or Lobed Leaves. Journal of Thermal Science and Technology, 2009; 4(1): 41-52.
[14] Shin'ya Obara. Itaru Tanno and Taichiro Shiratori, Light-receiving characteristics of a distributed solar module with a plant shoot configuration. Renewable Energy 2009; 34(5): 1210-1226.
[15] Mikkola, M. Experimental studies on polymer electrolyte membrane fuel cell stacks, Master's thesis submitted in partial fulfillment of the requirements for the degree of Master of Science in Technology, Helsinki University of Technology; 2001.
[16] Ibaraki Prefecture Government Office of Education, “Modeling of hydrogen energy system,” High school active science project research report. Ibaraki, Japan; 2002 (In Japanese)
[17] Shin'ya OBARA and Itaru TANNO. Arrangement Analysis of Leaves Optimized on Photon Flux Density or Photosynthetic Rate. Journal of Computational Science and Technology 2008; 2(1): 118-129.
[18] NEDO Technical information data base, Standard meteorology and Solar radiation data (METPV-3), http://www.nedo.go.jp/database/index.html; 2009.
[19] Narita K. Research on unused energy of cold region cities and utilization for district heat and cooling, Ph.D. thesis, Hokkaido University, Sapporo, Japan; 1996.

Captions

Fig. 1　Proposed energy system

Fig. 2　Cell performance generated with hydrogen and oxygen. Operating temperature 333K.

Fig. 3　Insolation of the level surface in Sapporo

(a) Solar angle of the direction and elevation

(b) Solar insolation

Fig. 4　Coordinate system with a plant shoot model

Fig. 5　Coordinate system of a shoot and leaf model

(a) Rotation around x-axis

(b) Rotation around z-axis and base point of the leaf

(c) Ginkgo-biloba leaf model

(d) Coordinate of the surface element

Fig. 6　Chromosome code

Fig. 7　Calculation flow

Fig. 8　The number of light quanta emitted from the virtual radiation plate

Fig. 9　Power demand model

(a) Representative day in each month

(b) Representative day in February

(c) Representative day in August

Fig. 10　Simulation result of the light received density on the square leaf model

(a) Square leaf model

(b) Light received density

Fig. 11　Simulation of the light received density of the ginkgo-biloba shoot model in Sapporo

(a) January

(b) July

Fig. 12　Simulation results in January and July representative day

January. The area of the solar module is 57.5 m^2 (horizontal type) and 43.8 m^2 (Slope type).

(a) Load factor of PEFC in January

(b) Amount of the power generation of the solar module

(c) Amount of the power storage

(d) Consumption of the gas compressors

July. The area of the solar module is 17.5 m^2 (horizontal type) and 20.8 m^2 (Slope type).

(e) Load factor of PEFC

(f) Amount of the power generation of the solar module

(g) Amount of the power storage

(h) Consumption of the gas compressors

Fig. 13　Simulation results of the solar module with plant shoot configuration. The area of the solar module is 14.7 m^2 (in January) and 9.2 m^2 (in July).

(a) Amount of the power generation of the solar module

(b) Amount of the power storage

(c) Consumption of the gas compressors

Fig. 14　Arrangement results in January of the plant shoot model of ginkgo biloba

(a) January

(b) July

Table 1　Simulation conditions of the proposed system

Table 2　Simulation conditions of the plant shoot solar module

Table 3　Simulation results in the solar module area

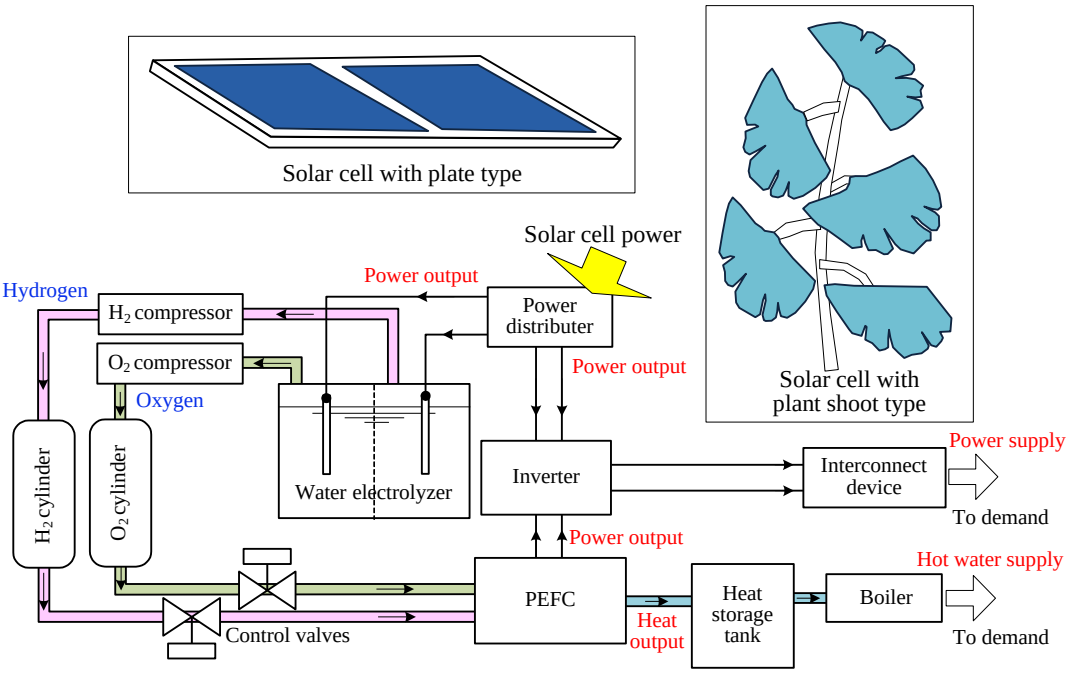

Fig. 1 Proposed energy system

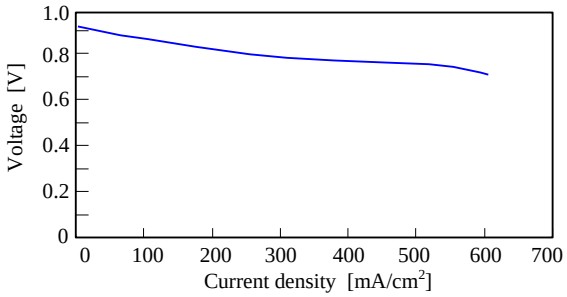

Fig. 2 Cell performance generated with hydrogen and oxygen. Operating temperature 333K.

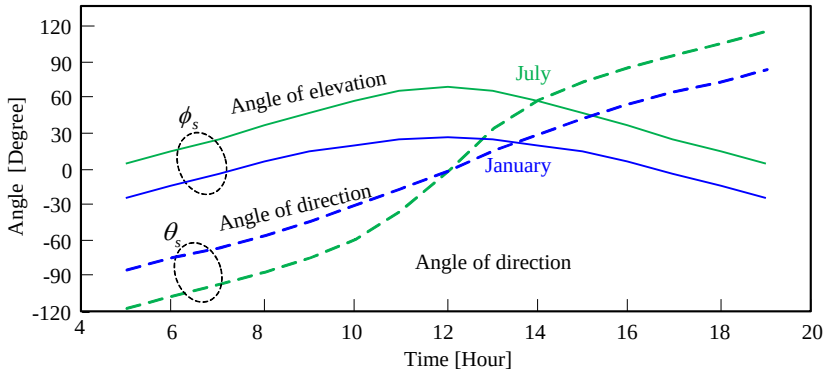

(a) Solar angle of the direction and elevation

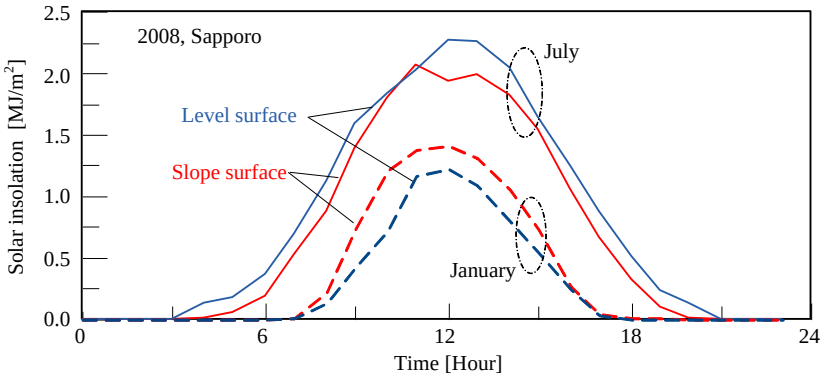

(b) Solar insolation

Fig. 3 Insolation of the level surface in Sapporo

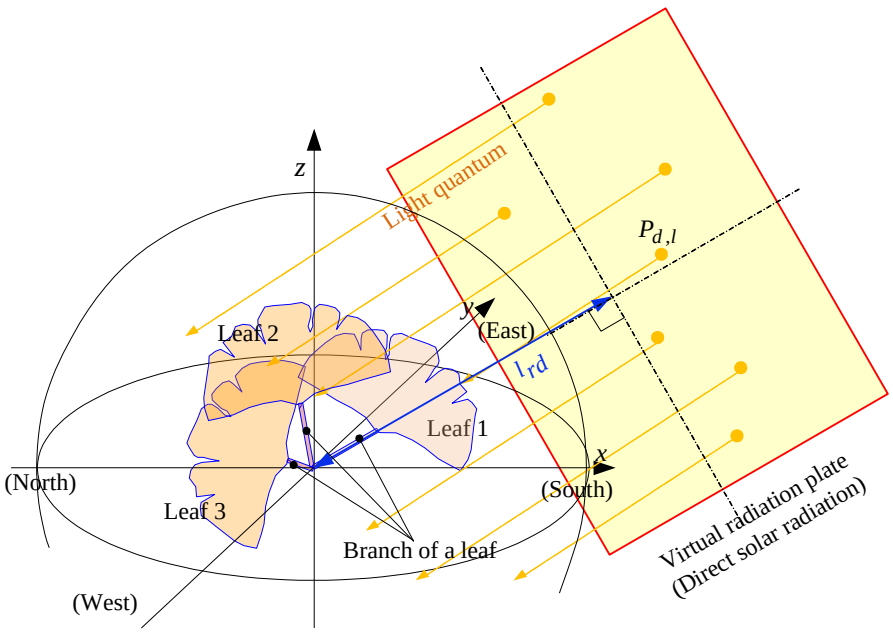

Fig. 4 Coordinate system with a plant shoot model

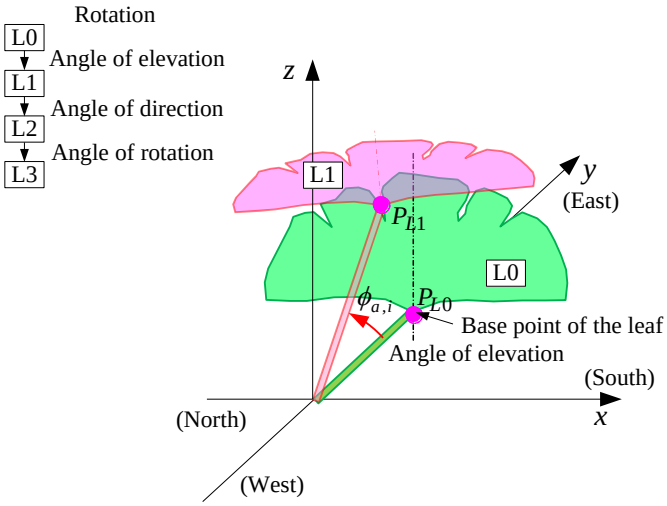

(a) Rotation around x-axis

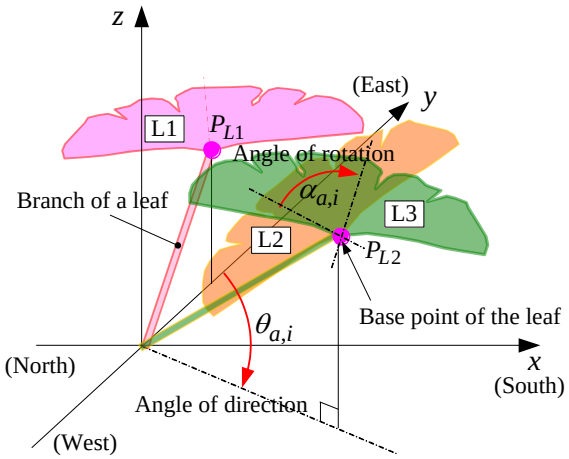

(b) Rotation around z-axis and base point of the leaf

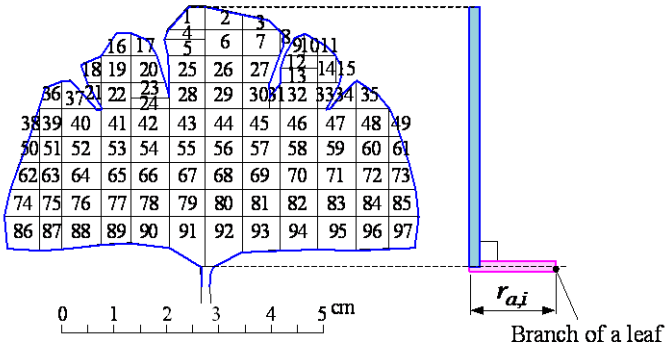

(c) Ginkgo-biloba leaf model

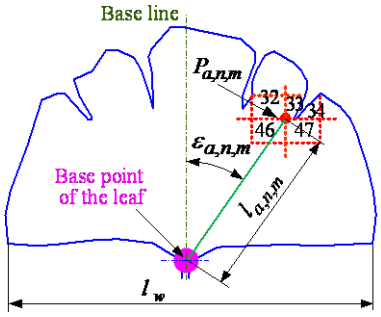

(d) Coordinate of the surface element

Fig. 5 Coordinate system of a shoot and leaf model

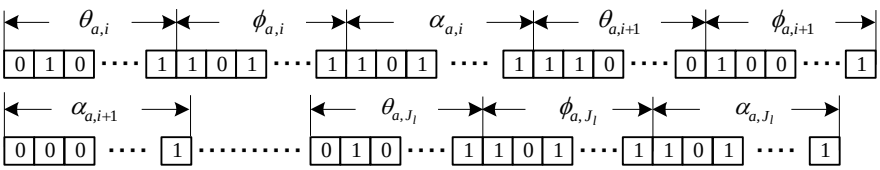

Fig. 6 Chromosome code

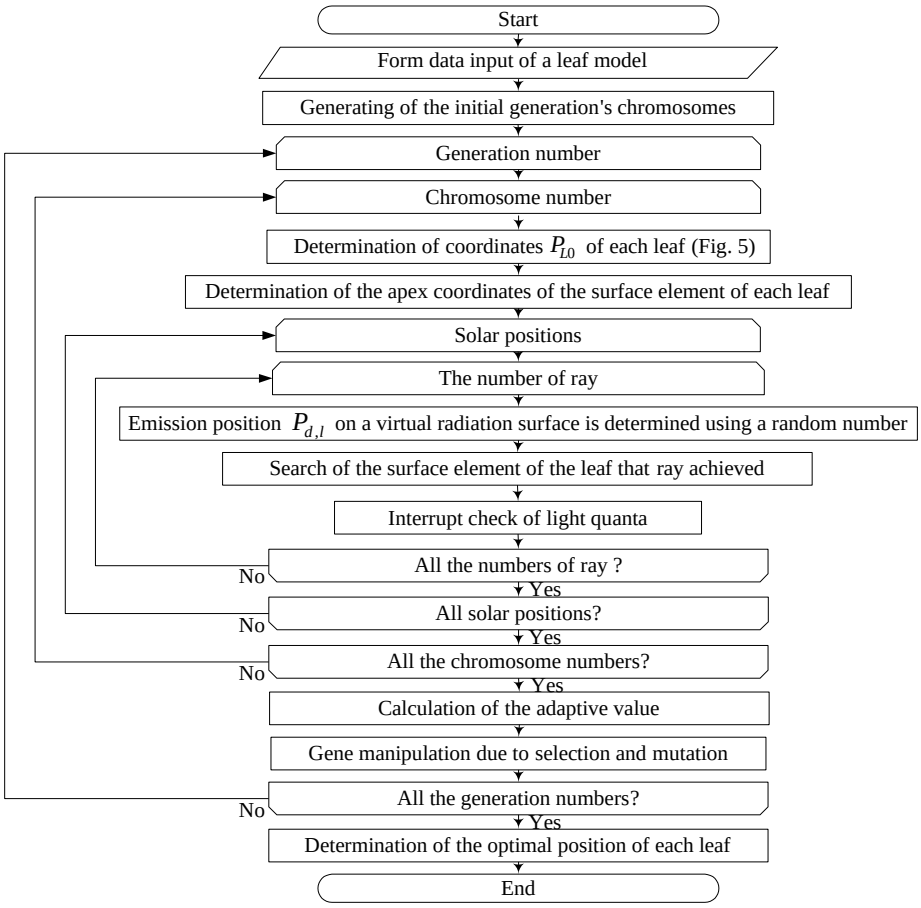

Fig. 7 Calculation flow

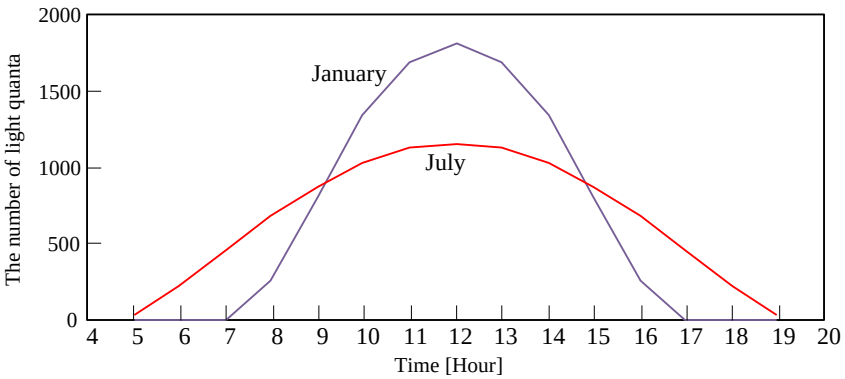

Fig. 8 The number of light quanta emitted from the virtual radiation plate

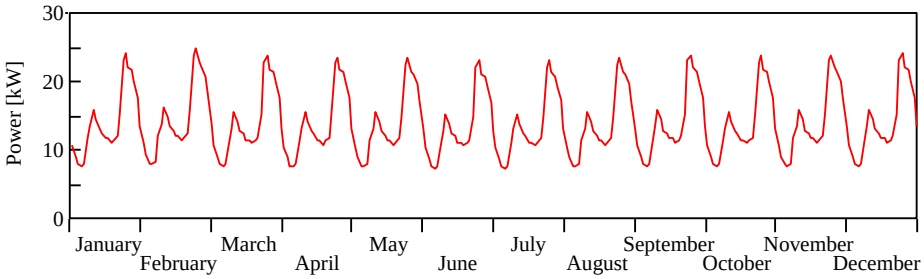

(a) Representative day in each month

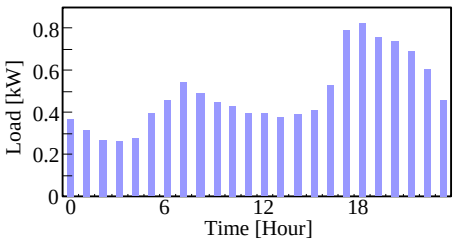

(b) Representative day in February

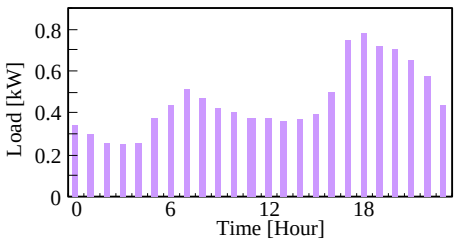

(c) Representative day in August

Fig. 9 Power demand model

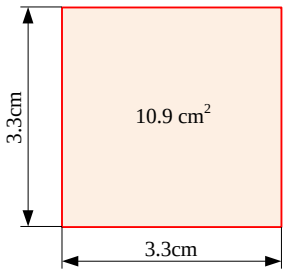

(a) Square leaf model

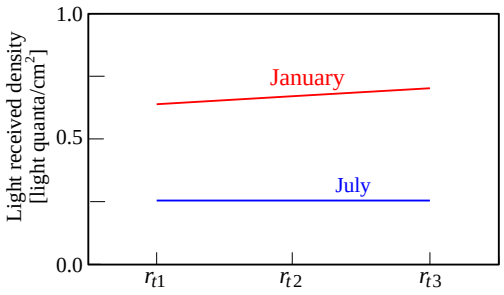

(b) Light received density

Fig. 10 Simulation result of the light received density on the square leaf model

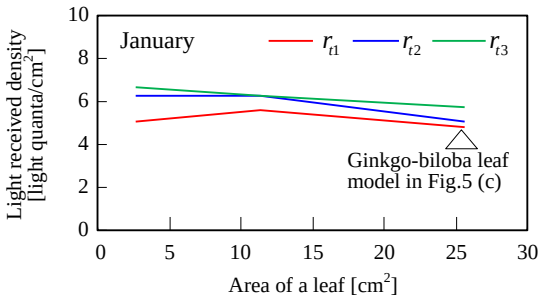

(a) January

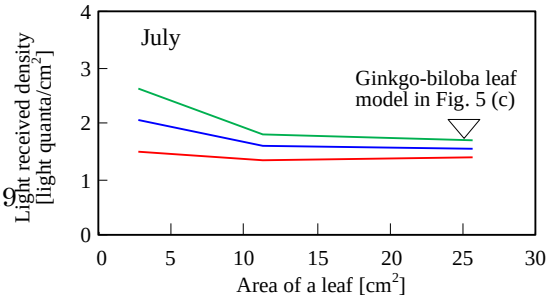

(b) July

Fig. 11 Simulation result of the light received density of the ginkgo-biloba shoot model in Sapporo

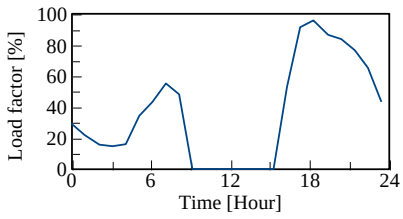

(a) Load factor of PEFC

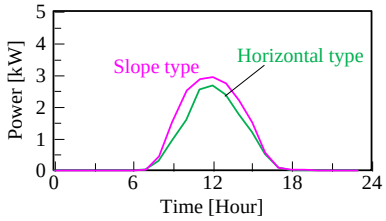

(b) Amount of the power generation of the solar module

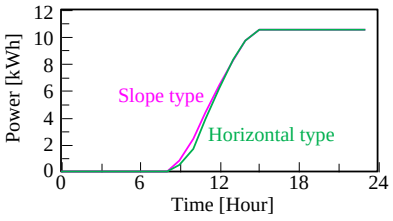

(c) Amount of the power storage

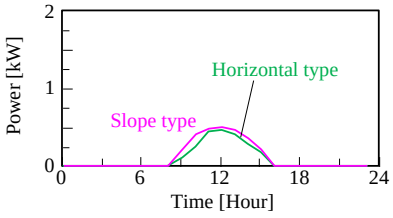

(d) Consumption of the gas compressors

January. The area of the solar module is 57.5 m^2 (horizontal type) and 43.8 m^2 (Slope type).

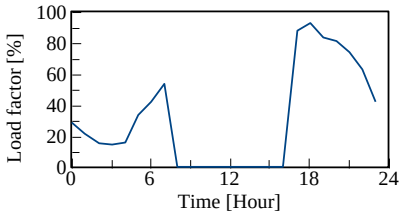

(e) Load factor of PEFC

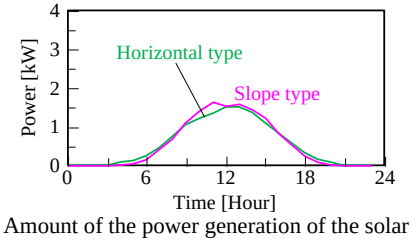

(f) Amount of the power generation of the solar module

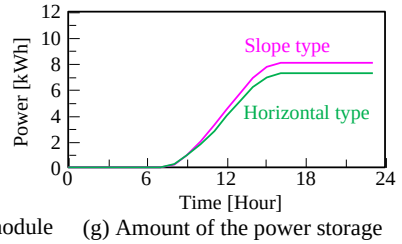

(g) Amount of the power storage

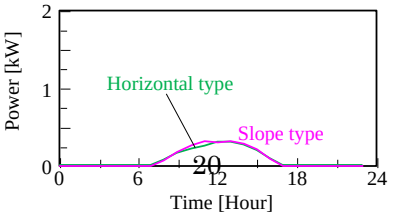

(h) Consumption of the gas compressors

July. The area of the solar module is 17.5 m^2 (horizontal type) and 20.8 m^2 (Slope type).

Fig. 12 Simulation results in January and July representative day

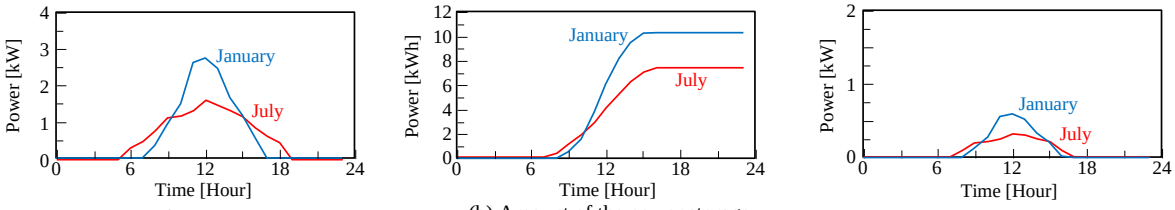

(a) Amount of the power generation of the solar module

(b) Amount of the power storage

(c) Consumption of the gas compressors

Fig. 13 Simulation results of the solar module with plant shoot configuration. The area of the solar module is 14.7 m^2 (in January) and 9.2 m^2 (in July).

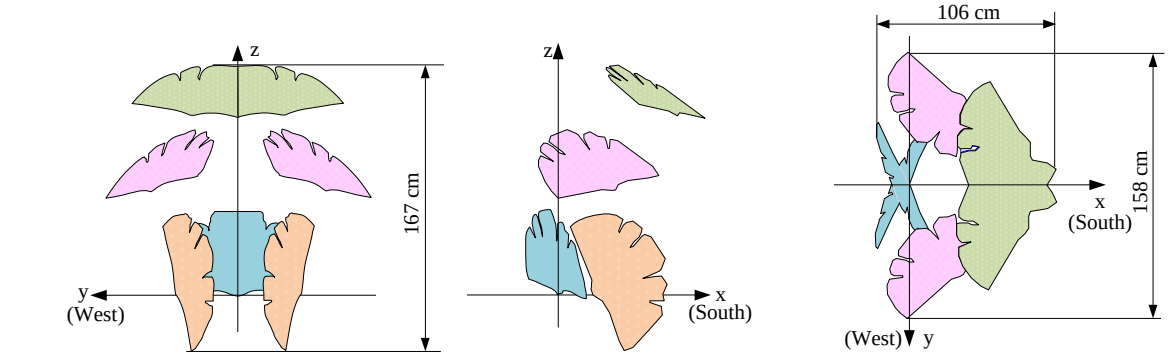

(a) January

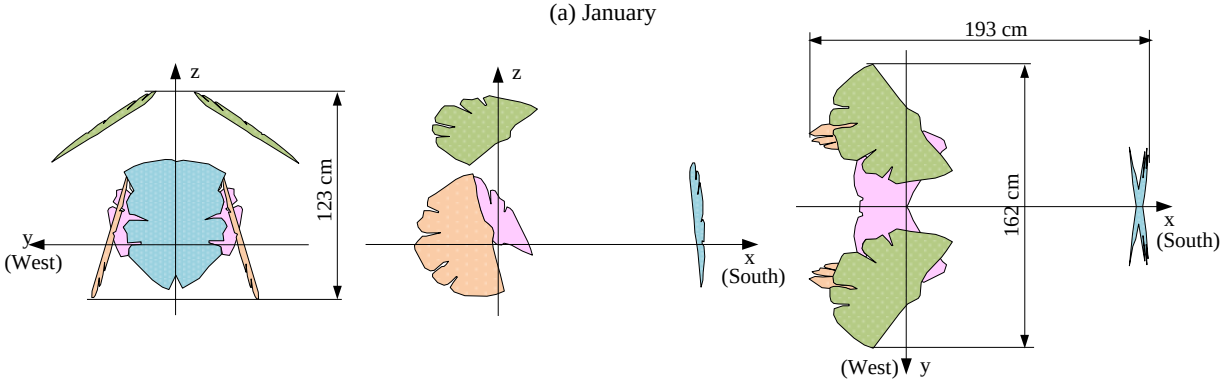

(b) July

Fig. 14 Arrangement results in January of the plant shoot model of ginkgo biloba

Table 1 Simulation conditions of the proposed system

Efficiency of solar module	14 %
Efficiency of the PEFC	55 %
Efficiency of the water electrolyzer	80 %
Efficiency of the compressor	50 %
Efficiency of the power conditioner (DC-AC converter and Inverter)	95 %
Storage pressure of hydrogen	0.5 MPa
Storage pressure of oxygen	0.5 MPa

Table 2 Simulation conditions of the plant shoot solar module

Leaf model : Ginkgo biloba (Fig. 6) The number of leaves : 4 Length of the branch of the leaf : 0, 30, 60, 90 mm Size of the Virtual radiation surface : Width and height 1000mm The number of the light quanta（direct light only）: 10000	Distance between the virtual radiation surface and the coordinate system center (Fig. 4): 500mm GA parameters Selection : Top 15 chromosomes Probability of the mutation : 0.2 The number of chromosome models : 100 Last generation number : 40

Table 3 Simulation results in the solar module area

Horizontal type	: January 57.5 m^2	July 17.5 m^2
Slope type	: January 43.8 m^2	July 20.8 m^2
Plant shoot configuration type	: January 14.7 m^2	July 9.2 m^2